ORNL/TM-2018/827

Neutron Residual Stress Mapping for Spent Nuclear Fuel Storage Canister Weldment

Jy-An John Wang
Andrew Payzant
Jeffrey Bunn
Ke An

April 20, 2018

OAK RIDGE NATIONAL LABORATORY
MANAGED BY UT-BATTELLE FOR THE US DEPARTMENT OF ENERGY

ORNL/TM-2018/827

NEUTRON RESIDUAL STRESS MAPPING FOR SPENT NUCLEAR FUEL STORAGE CANISTER WELDMENT

Jy-An John Wang[1], Andrew Payzant[2], Jeffrey Bunn[2], Ke An[2]

[1]Materials Science & Technology Division
[2]Neutron Scattering Division

Oak Ridge National Laboratory

Program Manager
Bruce Bevard, John Scaglione

Date Published: April 2018

Prepared by
OAK RIDGE NATIONAL LABORATORY
Oak Ridge, Tennessee 37831-6283
managed by
UT-BATTELLE, LLC
for the
U.S. DEPARTMENT OF ENERGY
under contract DE-AC05-00OR22725

CONTENTS

LIST OF FIGURES v
LIST OF TABLES vii
ACKNOWLEDGMENTS ix
ABSTRACT xi
1. INTRODUCTION 1
1.1 Background 1
1.2 Proposed experiment 2
1.3 the Origin of the received Sandia Mockup Canister Weldment 3
2. CANISTER WELDMENT RESIDUAL STRESS EVALUATION RESEARCH 7
2.1 d0 sample preparation 7
3. NEUTRON RESIDUAL STRESS MAPPING EXPERIMENT 9
4. NEUTRON DATA ANALYSES AND RESIDUAL STRESS EVALUATION 11
4.1 Basic Concept of Measuring Residual Strain by Neutron Diffraction Strain Mapping 11
4.2 Experimental Set-up and the Test Results 12
5. CONCLUSION 21

LIST OF FIGURES

Figure **Page**

Figure 1 Cross section of a longitudinal weld. Note that the outer diameter FZ passes well into the initial weld made on the inner diameter. Also note that the final weld passes were sometimes offset from the centerline of the weldment, yielding an asymmetric appearance.[1] 2

Figure 2 Dimensions of the received weld plate sectioned from Sandia full scale mockup SNF storage canister. Weld fusion region is about 28mm shown located in the middle of the weld plate. 3

Figure 3 The schematic diagram of the physical location of the received weldment, the axial weldment sample was used in neutron residual stress mapping study indicted with a purple arrow marker.[1] 4

Figure 4 Mockup container before being sectioned. (a) Location of these sections into which container was cut – one for residual stress analyses (A) and two for specimens (B and C). A temporary spider (b) was placed just below the cut made between sections A and B to minimize distortion as the cut was made. [1] 4

Figure 5 Location of surface strain gage positions along the longitudinal and circumferential welds as well as the position of temporary mounting blocks welded to the base of the container that facilitated positioning while the cuts were being made. [1] 5

Figure 6 Contour map across a longitudinal (axial) weld. Primary stress illustrated is the axial stress (parallel to the weld direction). The cross section is 400mm in length, and centered around the weld centerline. Red yellow represents tensile stresses, while green and blue represent compressive stresses. The through-wall tensile stress field extends approximately 25mm from the weld centerline 5

Figure 7 ICHD (a) and iDHD (b) data as a function of distance from the outer diameter of the container for the centerline of a longitudinal weld. Note that because the weld is aligned parallel to the long axis of the container, axial stresses are now parallel to the weld centerline 6

Figure 8 Comparison of the contour data for the axial stress measured via the deep hole drilling technique at a longitudinal weld for the (a) weld centerline and (b) HAZ.[1] 6

Figure 9 The detailed drawing of the D0 sample preparation, the dimensions are in mm 7

Figure 10 D0 sample was cut from the middle of the weldment, the area covered base metal, HAZ, and FZ. Three layers of such d0 samples were prepared and bonded with epoxy to form one single entity as shown above. (Top) d0 samples sectioned location, and (Bottom) final test sample set-up position for neutron scanning 8

Figure 11 (Top) Neutron residual stress mapping experimental set-up, and (Bottom) The detail of d0 and weld samples orientation during neutron beam scanning experiments 10

Figure 12 The schematic drawing of the neutron beam scanning contours at the middle plane throughout the thickness of the weldment 10

Figure 13 Neutron diffraction in a lattice structure. 11

Figure 14 Schematic diagram of neutron diffracted by the target material and using PSD detector to determine the peak angle, θ_{pk} 11

Figure 15 The measured residual strain plot and the estimate residual stress plot, along the 5 scanned contours in the hoop direction. Where the maximum residual tensile stress of 253 MPa is located at near the center of weld FZ 13

Figure 16 The estimate residual stress plot, along the five scanned contours in the radial direction; where the measured radial residual strain is near zero in the radial direction. Where the maximum residual tensile stress of 199 MPa is located at near the center of weld FZ 14

Figure 17 The measured residual strain plot and the estimate residual stress plot, along the five scanned contours in the axial direction. Where the maximum residual tensile stress of 439 MPa is located at near the center of weld FZ 15
Figure 18 2-D strain and stress contour plots in Hoop direction. 16
Figure 19 2-D strain and stress contour plots in Axial direction. 17
Figure 20 3-D strain and stress contour plots in Hoop direction. 18
Figure 21 3-D strain and stress contour plots in Axial direction. 19
Figure 22 Misalignment of the fusion zone centerline and boundary along the OD and ID of the weldment 20

LIST OF TABLES

Table **Page**

Table 1 Composition of the 304L plate and the 308L filler metal used for construct mockup. 2
Table 2 Stainless Steel Properties 2
Table 3 Proposed neutron residual stress mapping experimental plan 3

ACKNOWLEDGMENTS

This research was sponsored by the Spent Nuclear Fuel Canister Program of the US Department of Energy and was carried out at Oak Ridge National Laboratory under contract DE-AC05-00OR22725 with UT-Battelle, LLC.

The authors would like to thank Program Managers Bruce Bevard and John Scaglione for providing guidance and support to this project, Charles Bryan of Sandia National Laboratory for providing weldment samples, Randy Parton for d0 samples preparation, Lianshan Lin and Stylianos Chatzidakis for reviewing the report, and Sandy McPherson for providing editorial review.

ABSTRACT

Many radioactive materials within the nuclear fuel cycle present a significant hazard. Such materials include spent nuclear fuel, high-level waste, legacy waste and other nuclear materials that have no current outlet than storage. These materials are often held in long-term storage as an interim stage within their lifecycle. Lifecycles can include reuse or disposal. Safety and security of spent nuclear fuel (SNF) interim storage installations are very important, due to a great concentration of fission products, actinides and activation products. Stress corrosion cracking of interim storage containers has been identified as a high priority data gap by the Department of Energy. However, little has been done with regards to the canister weld material properties and their impact on stress corrosion, until recently from Sandia National Laboratory canister mockup program. Furthermore, because no post-weld heat treatment was required, the associated high tensile residual stress within these canister welds can drive the initiation and growth of stress corrosion cracking (SCC) cracks. In this work, we carried out in-situ neutron residual stress mapping on a weld plate sectioned from Sandia mock-up canister wall. Significant residual stress profiles were identified from the received longitudinal weld sample. The details of the weldment residual stress program development at ORNL are presented in this progress report. The generated residual stress profile from neutron diffraction technique is similar to that of Sandia residual stress data obtained from the deep hole drilling approach.

1. INTRODUCTION

1.1 BACKGROUND

Many radioactive materials within the nuclear fuel cycle present a significant hazard. Such materials include spent nuclear fuel, high-level waste, legacy waste and other nuclear materials that have no current outlet than storage. These materials are often held in long-term storage as an interim stage within their lifecycle. Lifecycles can include reuse or disposal. Safety and security of spent nuclear fuel (SNF) interim storage installations are very important, due to a great concentration of fission products, actinides and activation products. Stress corrosion cracking of interim storage containers has been indicated as a high priority data gap by the Department of Energy. However, little has been done regarding the canister weld material properties and their impact on stress corrosion, until recently with Sandia canister mockup program[1]. Furthermore, because no post-weld heat treatment was required, the associated high tensile residual stress within these canister welds can drive the initiation and growth of SCC cracks. In this work, we carried out in-situ neutron residual stress mapping on a received mock-up canister weldment form Sandia.

SCC of interim storage containers has been identified as a high priority data gap by the Nuclear Waste Technical Review Board[2], Department of Energy[3], the Nuclear Regulatory Commission[4,5], and the Electric Power Research Institute[6]. Uncertainties exist both in the understanding of the environmental conditions on the surface of the storage canisters and in the textural, microstructural, and electrochemical properties of the storage containers themselves. For an SCC crack to initiate, the tensile stresses in the metal must be of a sufficiently large magnitude that the threshold stress intensity value at a potential nucleation site is exceeded. The canister surface environment and the associated residual stress profiles have been evaluated by Sandia and EPRI[1,7,8], however, more needs to be done to assess canister material properties and their impact on corrosion. Of specific interest are regions associated with the welds on the canisters, because the welding process modifies the microstructure of the stainless steel as well as its resistance to localized corrosion. In addition, welding introduces high tensile residual stresses that can drive the initiation and growth of SCC cracks.

To meet the need for additional data on the canister material properties, the DOE Used Fuel Disposition campaign program has procured a full-diameter cylindrical mockup of a dual certified 304/304L stainless steel (SS) storage canister produced using the same manufacturing procedures as fielded SNF fuel interim storage canisters. ORNL recently received five such weld plates, three longitudinal welds and two circumferential welds. High residual tensile stresses may be present in the metal, due to cold working or welding. Weld residual stresses (WRS) are generally the most important component, and are a function of many factors, including weld geometry, sample thickness, welding speed, number of passes, inter-pass temperatures, and base metal properties relative to the weld. Because of this, WRS are specific to the geometry and welding processes used and can only be measured from an actual storage canister or a mockup made using the same procedures as the real canisters. While the residual stresses were anticipated to be largest in the weld fusion zone (FZ), the regions surrounding the weld (the HAZ) are the regions where localized corrosion is most likely to initiate due to sensitization resulting from the thermal profile associated with the welding process. Characterization of the stresses in the HAZ can be accomplished by performing neutron scattering measurements approximately 4 mm from the weld toe (i.e., edge of the weld FZ).

The compositions of the 304/304L SS plates and the 308L SS filler material used to build the mockup canister are listed in Table 1 below. All the welds of the mockup canister were formed via the submerged-arc welding (SAW) process with multi-pass welds.[1]

Table 1 Composition of the 304L plate and 308L filler metal used for construct mockup.

	C	Co	Cr	Cu	Mn	Mo	N	Ni	P	S	Si
Plate Material (304/304L)	0.0223	0.1865	18.1000	0.4225	1.7125	0.3180	0.0787	8.0270	0.0305	0.0023	0.2550
Weld Filler (308L) (lot 1)	0.014	--	19.66	0.16	1.70	0.11	0.058	9.56	0.025	0.010	0.39
Weld Filler (308L) (lot 2)	0.012	--	19.71	0.192	1.730	0.071	0.053	9.750	0.024	0.012	0.368

The inner diameter was welded first, followed by the outer diameter. Once the inner diameter weld was made, the edge preparation for the outer diameter weld was made by arc-gouging along the parting line between the two plates being welded together. A representative cross-sectional image of a circumferential weld is presented in Figure 1 below.

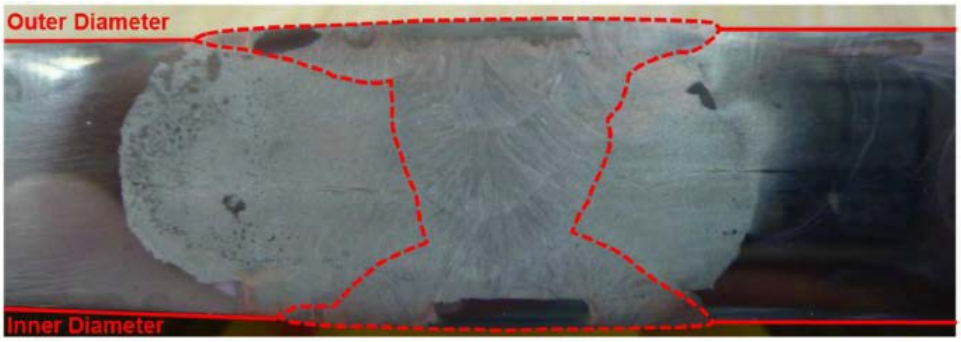

Figure 1 Cross section of a longitudinal weld. Note that the outer diameter FZ passes well into the initial weld made on the inner diameter. Also note that the final weld passes were sometimes offset from the centerline of the weldment, yielding an asymmetric appearance.[1]

The tensile properties of the 304, 304L, and 308L SS plates materials are stated in Table 2.[9]

Table 2 Stainless Steel Properties

Type	E [GPa]	0.2% Yield stress [MPa]	UTS [MPa]
304	195	241	586
304L	195	207	552
308L	195	207	551

1.2 PROPOSED EXPERIMENT

In this work, we propose to evaluate the residual stress profiles of base metal, weld FZ, and HAZ regions within the weld plate. Residual stresses in the weld plate would be measured by neutron diffraction at the High Flux Isotope Reactor, Neutron Residual Stress Mapping Facility (NRSF2). For NRSF2 the normal wavelength used is 0.189 nm. The hkl's Al [311] was measured at 101.5°. The gage volume was defined by a 1mm width x 10 mm height incident slit and 1mm width receiving slit when measuring TD and ND, and the height will be reduced 1mm when measuring LD. The strains will be measured at weld FZ, HAZ

and base metal regions on the weld plate, shown in Figure 2. Sample area far away from the weld FZ and HAZ will be taken as stress-free reference to calculate residual strains, and the residual stresses were calculated with Hook's Law based on a plane stress assumption.

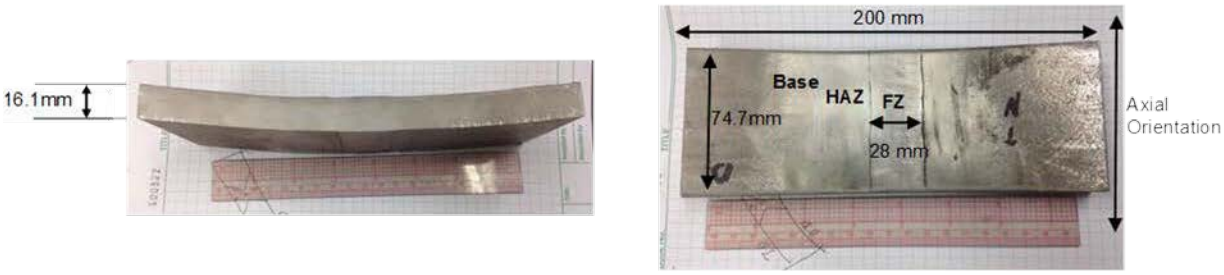

Figure 2 Dimensions of the received weld plate sectioned from Sandia full scale mockup SNF storage canister. Weld fusion region is about 28mm shown located in the middle of the weld plate.

The measurements of three zones, base metal, HAZ, and FZ, were performed on the received weld plate. Tests were performed in air at ambient temperature. The d0 sample was provided by slicing of the similar weld and perform similar mapping scheme but with measuring one direction. Due to multiple locations and welding zones across the weld plate, and set up times, it took a total period of five days beam time to complete the neutron scanning through five thickness locations of the weldment. The detailed experimental matrix is provided in Table 3.

Table 3 Proposed neutron residual stress mapping experimental plan.

Sample	Zone Locations x Thickness Locations x Axial Locations
Sample 1: FZ region	6 x 12 x 1
Sample 1: HAZ region	6 x 12x 1
Sample 1: Base metal region	3 x 4 x 3
	Total measurements points 152x3 directions + d0 (152)

Neutron diffraction at HFIR is preferred for this experiment because neutrons are superior to x-rays in terms of the penetration depth and the large sample volume that can be probed by the neutron beam. The details of the neutron residual stress mapping program development are presented in the following sections.

1.3 THE ORIGIN OF THE RECEIVED SANDIA MOCKUP CANISTER WELDMENT

The received canister weldment samples are from the top portion of the Cut B section, as shown in Figure 3 with purple arrow marker. The picture of the associated Sandia markup canister and the marked cut sections of A, B, and C is shown in Figure 4, where Section A is for residual stress analyses, B section is for weld samples, and C section is for NDE evaluation.

The details of strain gages locations in Section A are shown in Figure 5. The residual stress contour map across the longitudinal (axial) weld is shown in Figure 6. The axial and hoop residual stress measurements from the deep hole drilling method are illustrated in Figure 7. The comparison of Sandia's deep hole drilling measurements and contour data in the longitudinal weld is shown in Figure 8 for the FZ and HAZ zones. The contour map and the deep hole drilling data appeared to be quite consistent in the weld fusion zone region; and the deep hole drilling data indicates that the maximum tensile residual stress is about 423

MPa near the weld centerline. The tensile residual stress profile at the HAZ region is also much lower than that of the FZ region.

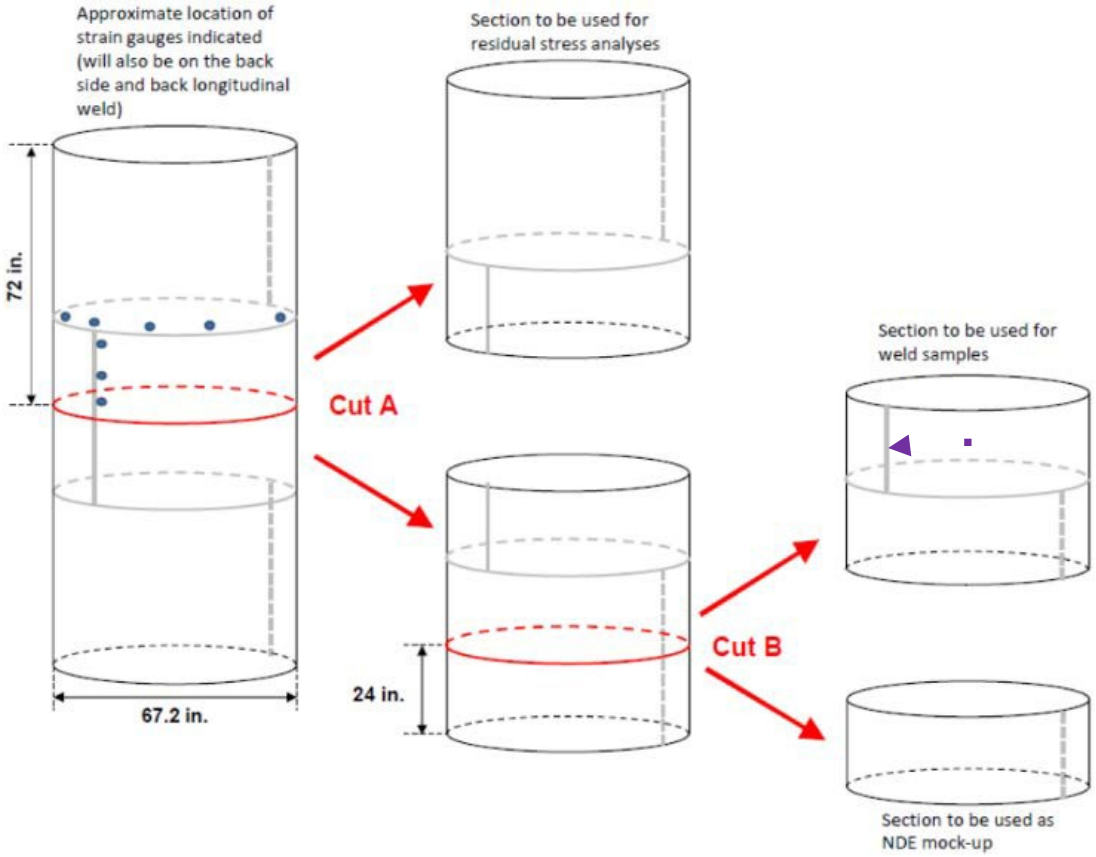

Figure 3 The schematic diagram of the physical location of the received weldment, the axial weldment sample was used in neutron residual stress mapping study indicted with a purple arrow marker.[1]

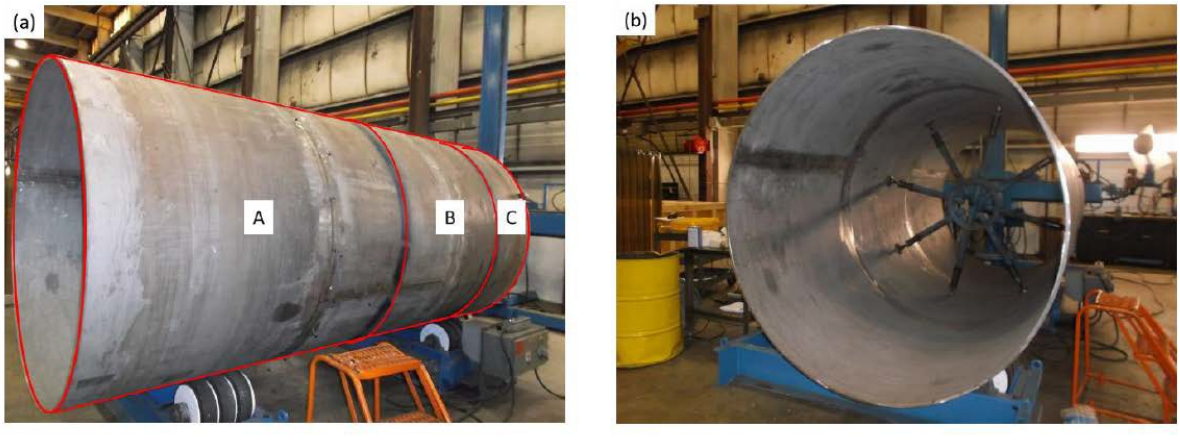

Figure 4 Mockup container before being sectioned. (a) Location of these sections into which container was cut – one for residual stress analyses (A) and two for specimens (B and C). A temporary spider (b) was placed just below the cut made between sections A and B to minimize distortion as the cut was made. [1]

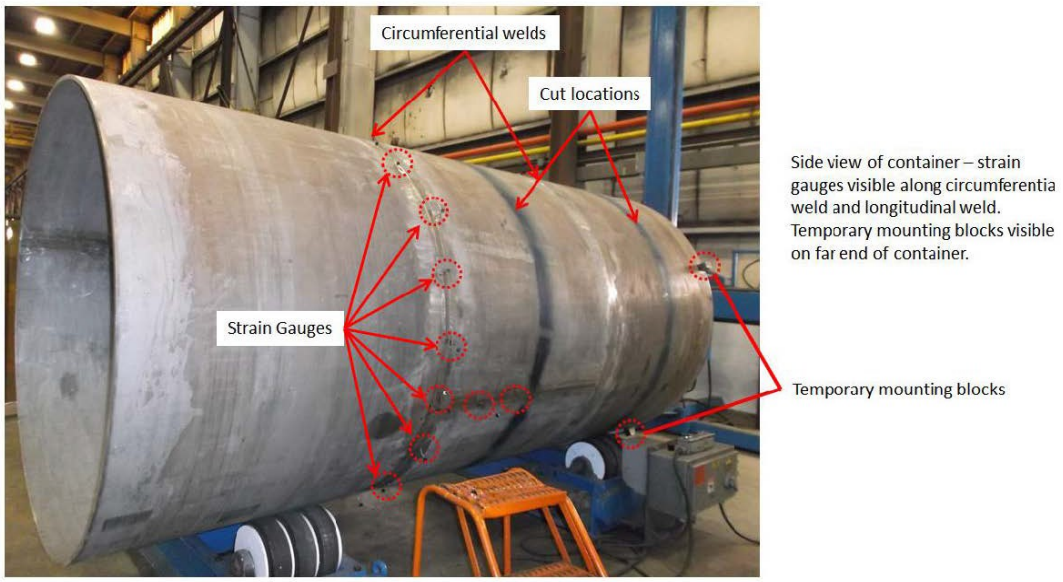

Figure 5 Location of surface strain gage positions along the longitudinal and circumferential welds as well as the position of temporary mounting blocks welded to the base of the container that facilitated positioning while the cuts were being made. [1]

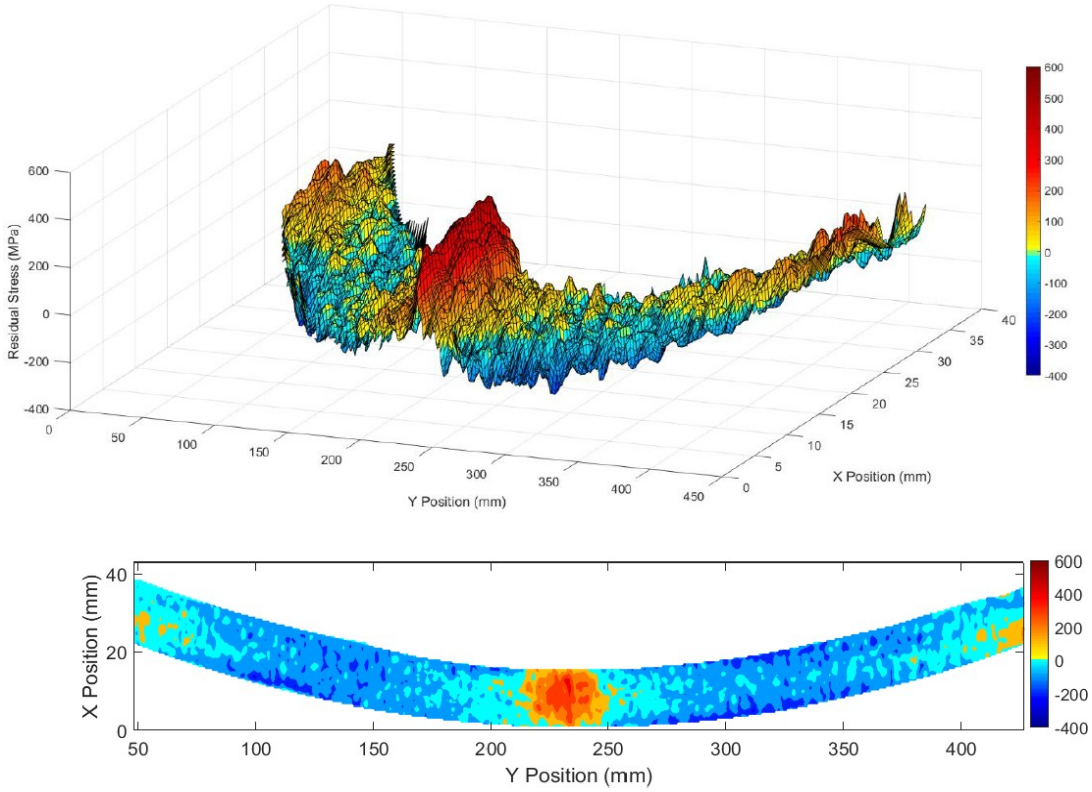

Figure 6 Contour map across a longitudinal (axial) weld. Primary stress illustrated is the axial stress (parallel to the weld direction). The cross section is 400mm in length, and centered around the weld centerline. Red yellow represents tensile stresses, while green and blue represent compressive stresses. The through-wall tensile stress field extends approximately 25mm from the weld centerline.

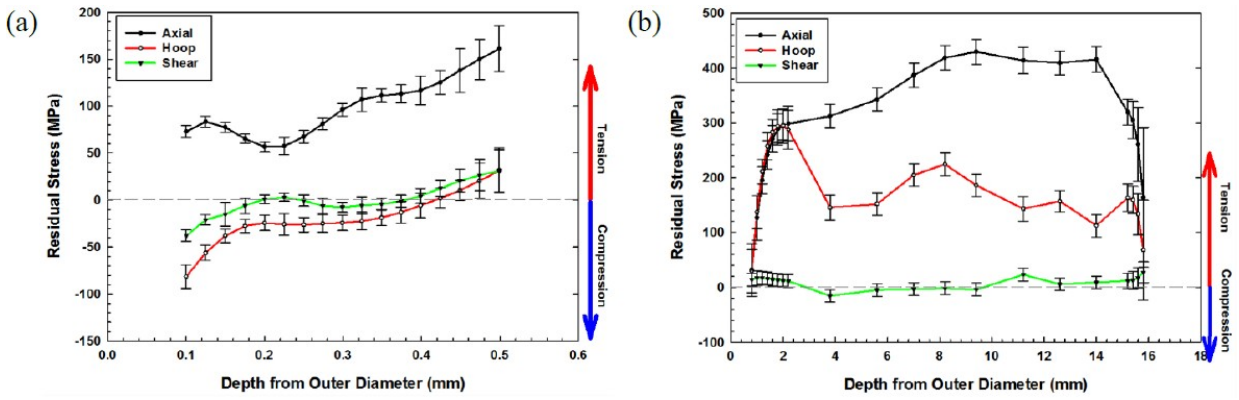

Figure 7 ICHD (a) and iDHD (b) data as a function of distance from the outer diameter of the container for the centerline of a longitudinal weld. Note that because the weld is aligned parallel to the long axis of the container, axial stresses are now parallel to the weld centerline.

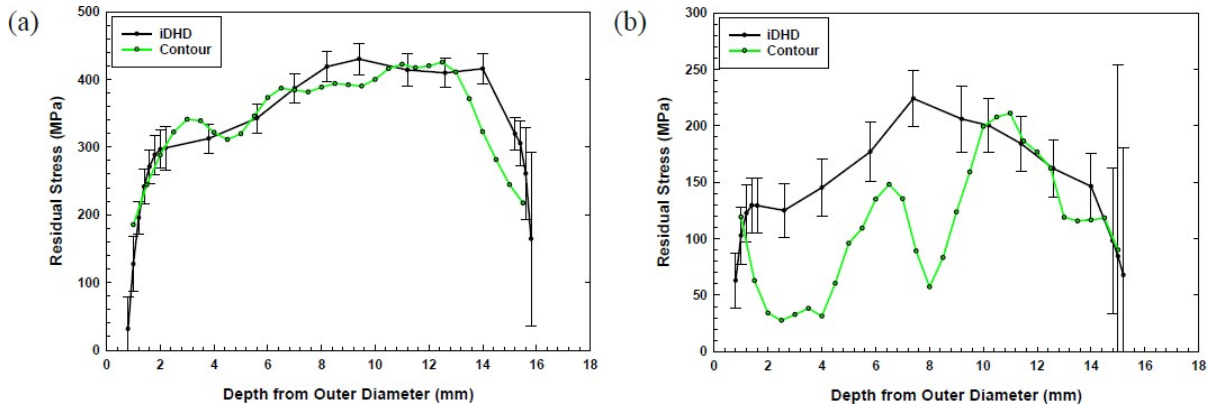

Figure 8 Comparison of the contour data for the axial stress measured via the deep hole drilling technique at a longitudinal weld for the (a) weld centerline and (b) HAZ.[1]

2. CANISTER WELDMENT RESIDUAL STRESS EVALUATION RESEARCH

Residual stress is generated in the structures as a result of irregular elastic–plastic deformation during fabrication processes such as welding, heat treatment, and mechanical processing. Where the mechanical forming process and welding were involved in canister manufacturing processes. There are several factors attributed to the origin of residual stresses, tensile or compressive. The stresses can be determined by destructive ways or non-destructive ways by using X-ray or neutron diffraction. We propose to use in-situ neutron diffraction technique to measure weldment's residual stress.

There are three major tasks to be performed during the program development, namely, (1) weldment d0 sample preparation, (2) neutron residual stress mapping experiment performed at HFIR NRSF2 facility, and (3) neutron scanning data analyses and the associated residual stress evaluations. The d0 sample preparation will be discussed in this section.

2.1 d_0 SAMPLE PREPARATION

The details of preparation procedure for making d0 sample is shown in Figure 9. The fine cutting is designed to release the existing residual stress within the metal plate. d_0 sample provides the baseline benchmark property of the parent weldment, which was cut from the parent weld plate as detailed in Figure 10.

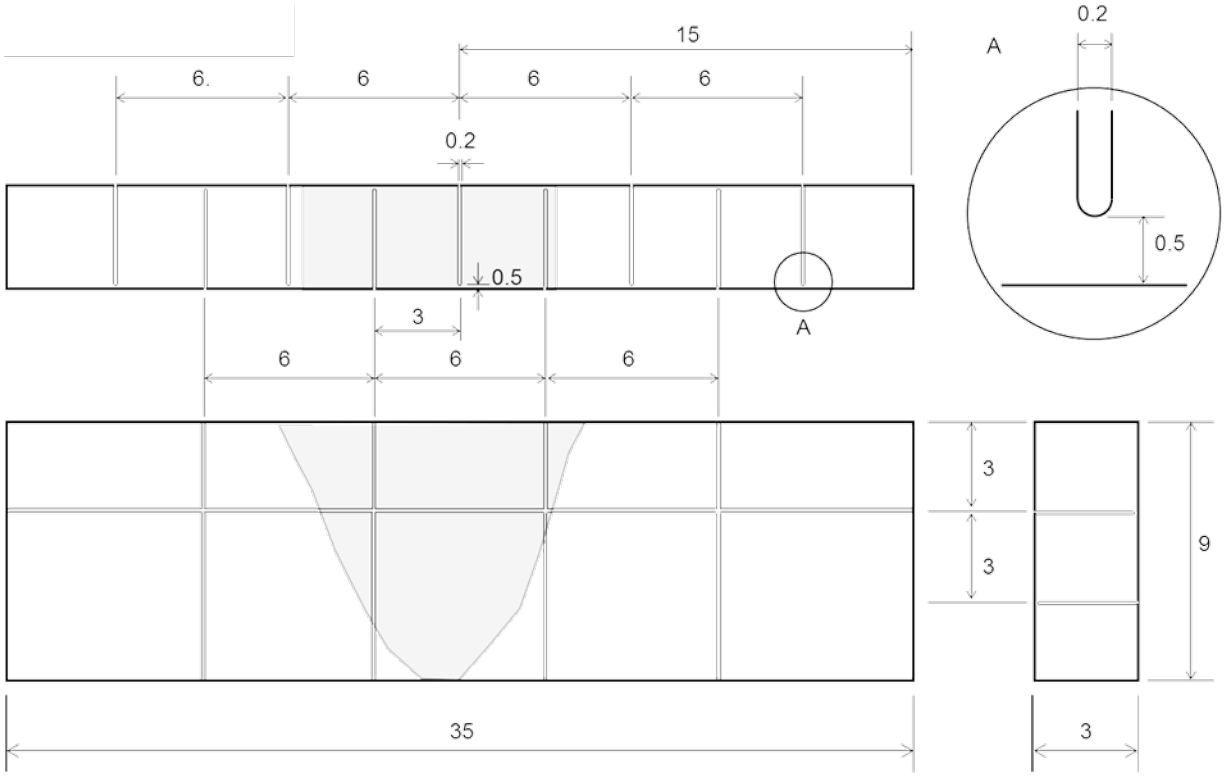

Figure 9 The detailed drawing of the D0 sample preparation, the dimensions are in mm.

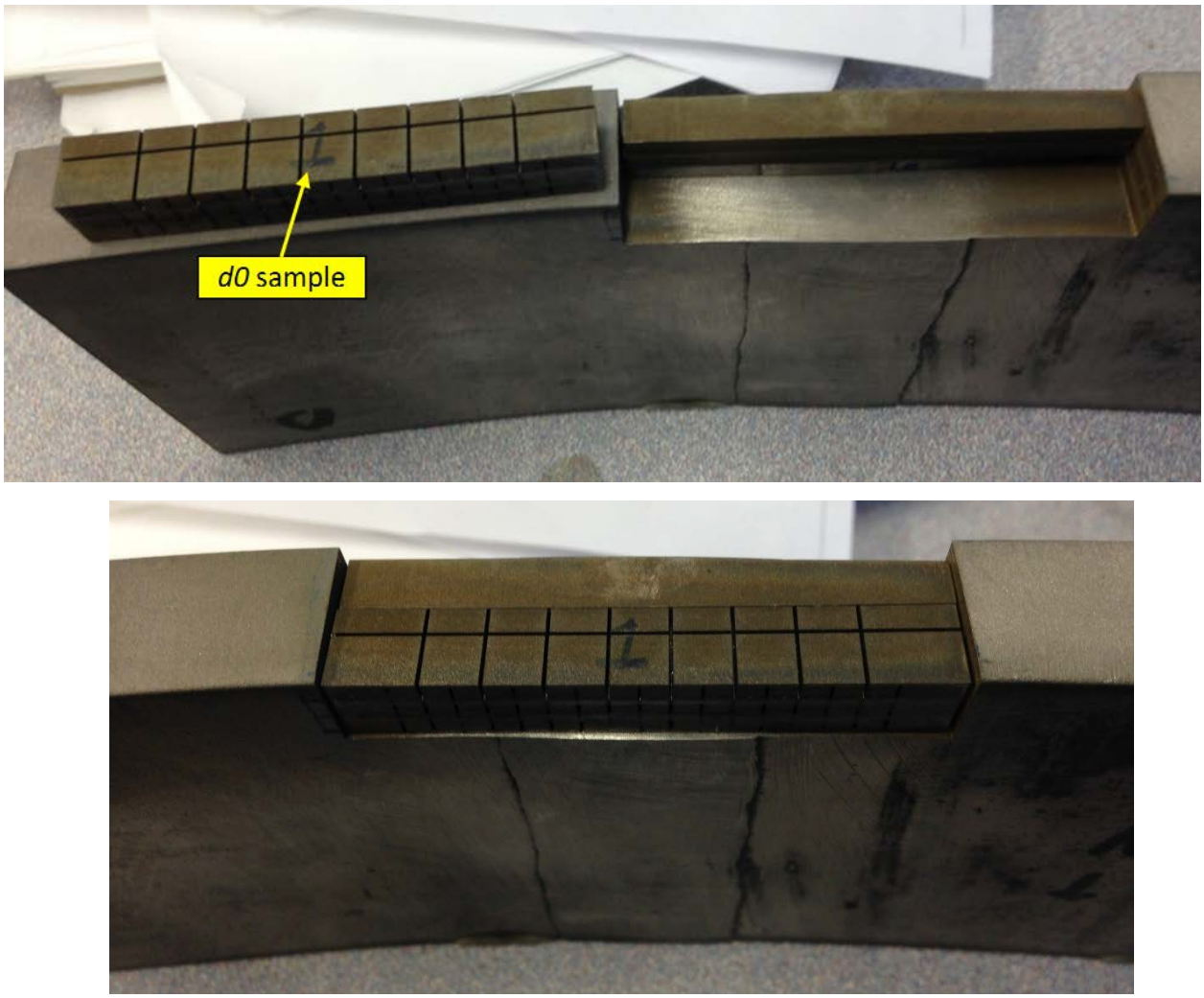

Figure 10 d_0 sample was cut from the middle of the weldment, the area covered base metal, HAZ, and FZ. Three layers of such d0 samples were prepared and bonded with epoxy to form one single entity as shown above. (Top) d0 samples sectioned location, and (Bottom) final test sample set-up position for neutron scanning.

3. NEUTRON RESIDUAL STRESS MAPPING EXPERIMENT

In order to benchmark the residual stress profile within the received weldment, a non-destructive evaluation using neutron scattering technique for determining the residual stress profile within the weld plate was carried out. This neutron residual stress mapping experiment was carried out at ORNL High Flux Isotope Reactor (HFIR) Facility in November 2017. The NRSF2 highest flux research instrument and support at HFIR facility provides a unique capability and a state-of-the-art knowledge base for materials science research on measuring strains and strain gradients in materials. A 2θ goniometer with large XYZ/Ω mapping stages and a seven-detector array were provided at NRSF2, as illustrated in Figure 11. NRSF2 set-up has multiple wavelengths for different materials and can conduct measurements of strains for multiple (hkl)'s lattice plans. A 25kN linear electric actuator load frame allows in-situ neutron measurement under tensile or/and compressive load. The experiment was completed after five days of neutron beam time. In order to increase the strain mapping resolution, there are five trace lines through the weld sample thickness, shown in Figure 12, were scanned sequentially by neutron beam. Thus, a longer beam time was required for each targeted position, in order to have better resolution of residual strain mapping within the targeted base metal, HAZ, and FZ zones.

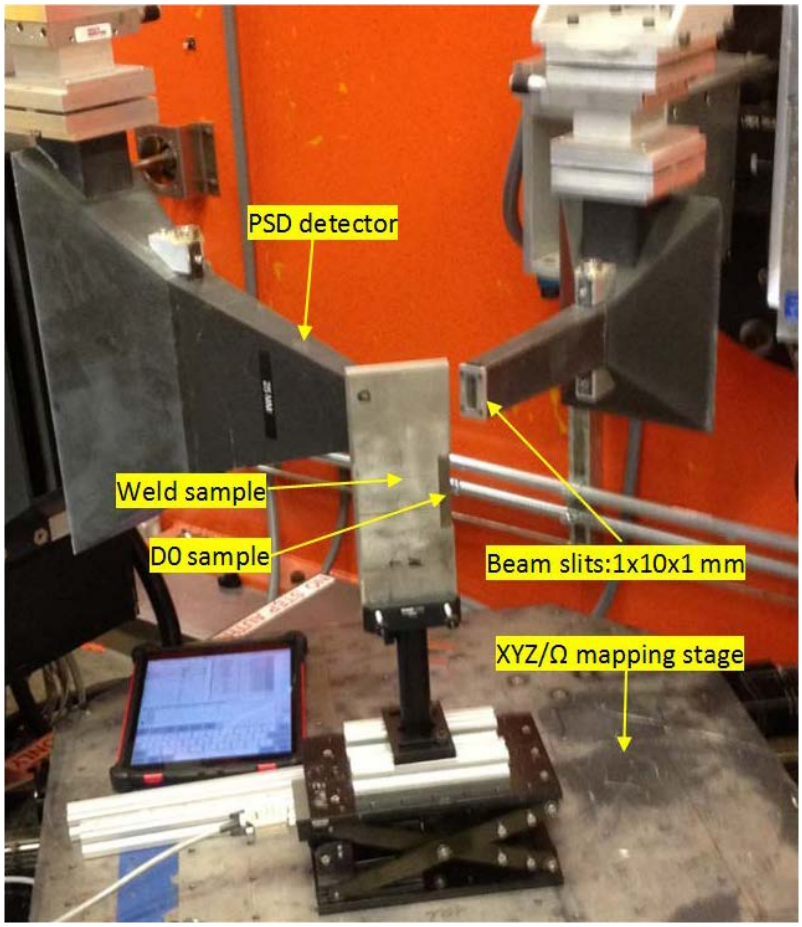

NRSF2 set-up with weld sample

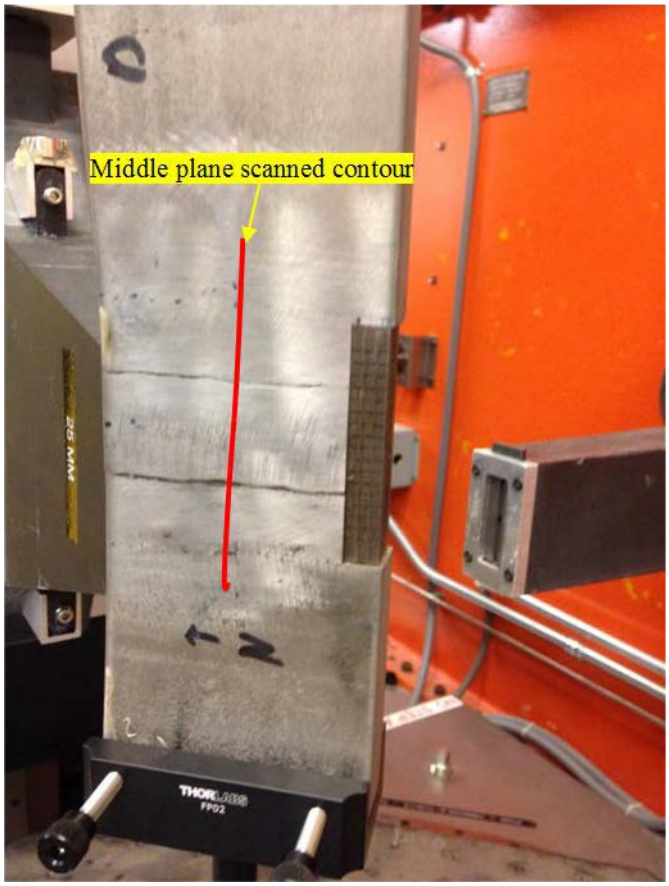

The details of D0 and weld sample

Figure 11 (Top) Neutron residual stress mapping experimental set-up, and (Bottom) The detail of d0 and weld samples orientation during neutron beam scanning experiments.

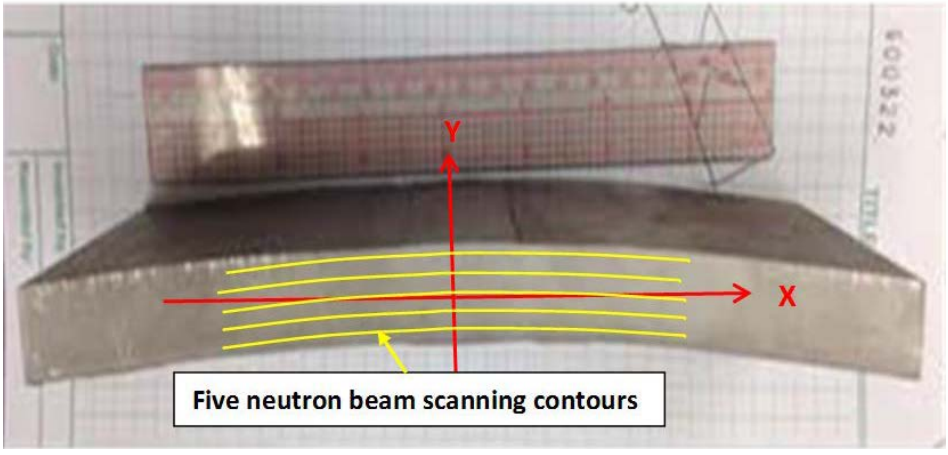

Figure 12 The schematic drawing of the neutron beam scanning contours at the middle plane throughout the thickness of the weldment.

4. NEUTRON DATA ANALYSES AND RESIDUAL STRESS EVALUATION

4.1 BASIC CONCEPT OF MEASURING RESIDUAL STRAIN BY NEUTRON DIFFRACTION STRAIN MAPPING

In a neutron scattering technique, the lattice spacing, d, is determined according to Bragg's Law as illustrated in the following formula and in Figures 13-14,

$$d = \frac{\lambda}{2\sin\theta_{pk}}$$

and, lattice strain is given by

$$\varepsilon = \frac{d - d_0}{d_0}$$

where, d_0 is the strain free d-spacing.

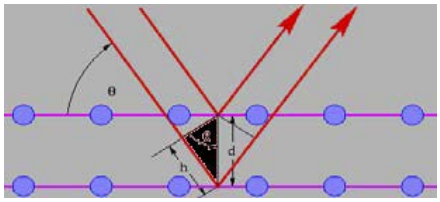

Figure 13 Neutron diffraction in a lattice structure.

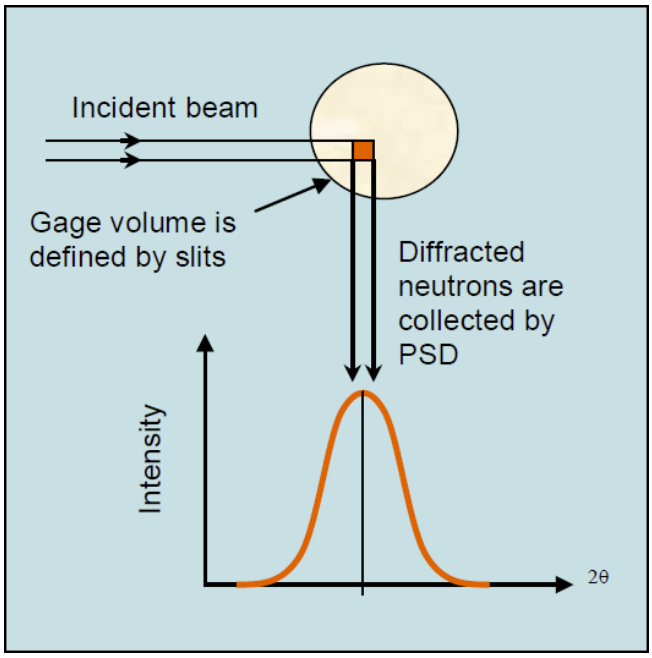

Figure 14 Schematic diagram of neutron diffracted by the target material and using PSD detector to determine the peak angle, θ_{pk}.

Upon determination of the residual strain in X, Y, and Z-coordinates, the residual principal stress can then be calculated according to Hooke's Law with three strain components as described below:

$$\sigma_x = \frac{E}{(1+\nu)(1-2\nu)}\left[(1-\nu)\varepsilon_x + \nu(\varepsilon_y + \varepsilon_z)\right]$$
$$\sigma_y = \frac{E}{(1+\nu)(1-2\nu)}\left[(1-\nu)\varepsilon_y + \nu(\varepsilon_x + \varepsilon_z)\right]$$
$$\sigma_z = \frac{E}{(1+\nu)(1-2\nu)}\left[(1-\nu)\varepsilon_z + \nu(\varepsilon_x + \varepsilon_y)\right]$$

In which E and υ are the appropriate values of Young's Modulus and Poisson's Ratio, respectively, for the crystallographic direction, *hkl*.

4.2 EXPERIMENTAL SET-UP AND THE TEST RESULTS

The detailed illustration of the weldment sample mounted at NRSF2 is shown in Figure 11. The tested samples, including d_0 and the weldment samples, the lattice plans, and neutron beam orientation and position of the test samples are outlined below,

- Sample: – d_0 and weldment samples
  – which covers the base metal, HAZ, and weld fusion zones.
- hkl's measured: Al [311] at 101.5°, Fe [211] at 107.7°
- Wavelength: 0.189 nm from monochromator Si400
- Slits: 1x10x1 mm
- Neutron beam scanning was performed along five contours at the middle plane of the weldment, shown in Figure 10 with blue markers on the weldment.
- Residual strains in X, Y, and Z directions along the five contours were measured.

The measured strains in the radial direction are near zero. Thus, the plane strain condition was justified to calculate the weldment's strain and stress accordingly in the hoop and axial directions. The details of the test results for the hoop (circumferential), radial, and axial (longitudinal) residual stresses profiles along the scanning contours are shown in Figures 15-17. The strain and stress profiles of 2-D and 3-D contour plots are shown in Figures 18-21.

Over the measured area along the circumferential direction of the longitudinal weld, the residual forces do not balance, due to the limited range of scanned area covered into the base metal. The balancing forces are outside the measured area.

The strain data has significant scatter in the weld region, as well as in d_0 specimens; however, it appears to be less scatter in the base metal. This is primary due to the fact that the weld region has comparatively large grains, or large dendrites, or both. Thus, a 3-point average was adopted to smooth the results, and this yielded much more sensible data as presented in the plots.

The estimated maximum axial tensile stress is 439 MPa located near the centerline of the weld. This value is comparable to estimates reported by Sandia estimate for the maximum axial tensile residual stress near the centerline of the longitudinal weld.

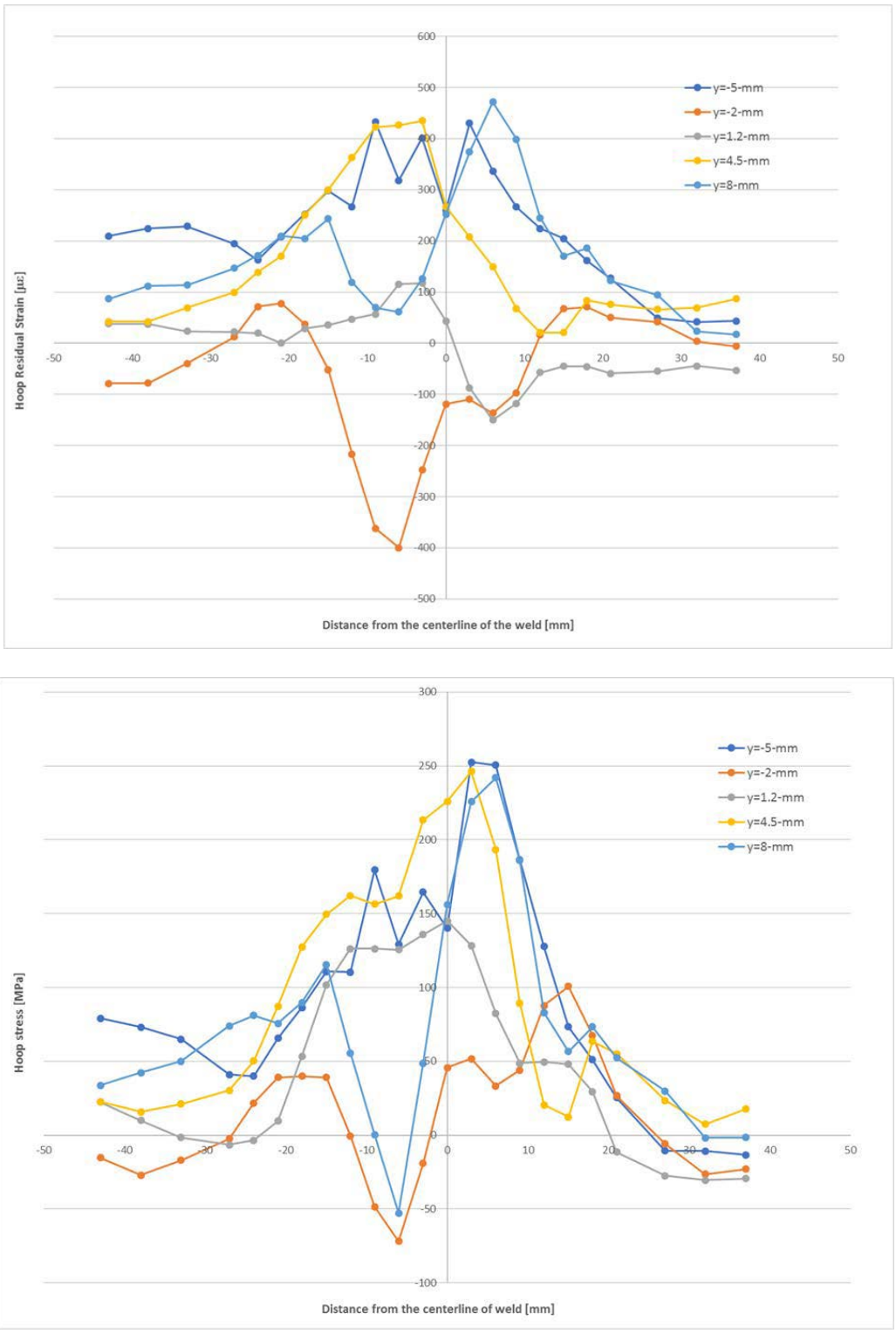

Figure 15 Measured residual strain plot and the estimate residual stress plot, along the 5 scanned contours in the hoop direction. Where the maximum residual tensile stress of 253 MPa is located at near the center of weld FZ.

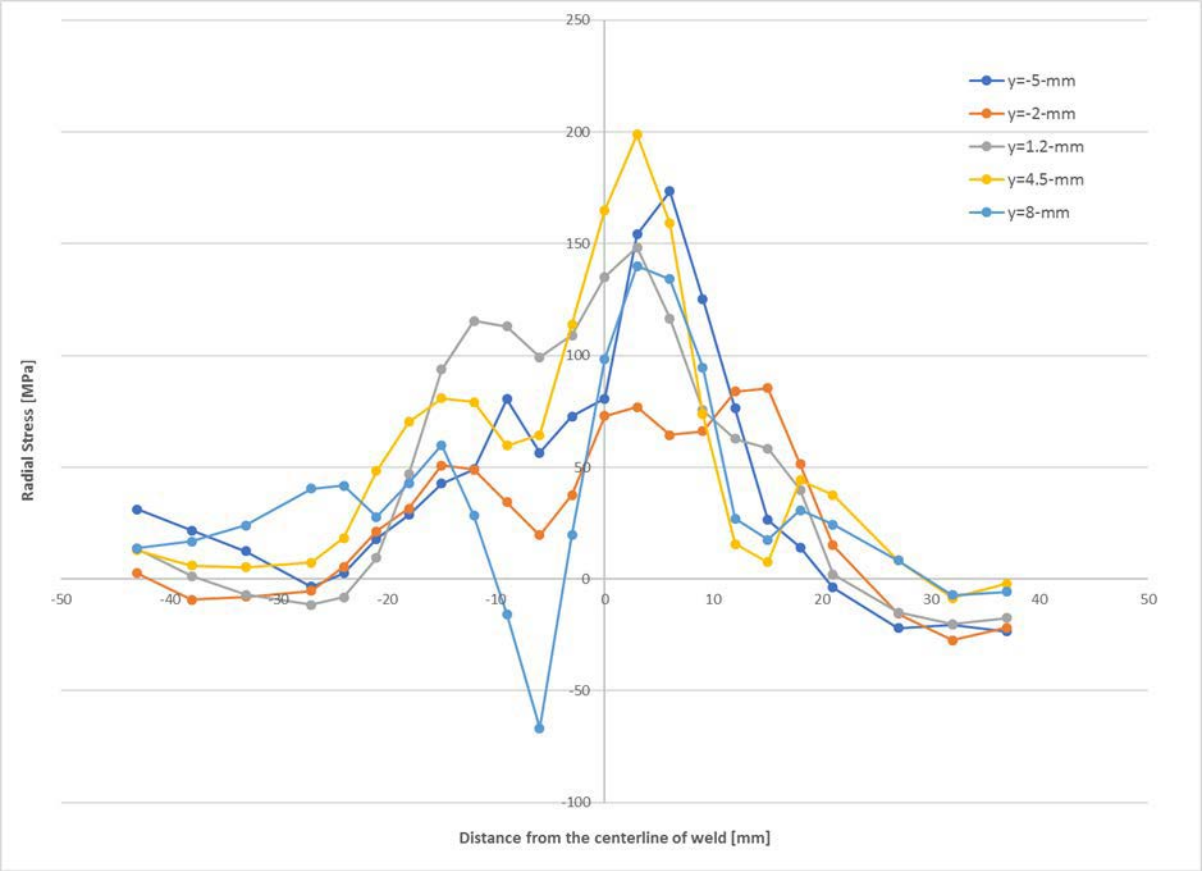

Figure 16 The estimated residual stress plot, along the five scanned contours in the radial direction; where the measured radial residual strain is near zero in the radial direction. The magnitude of the maximum residual tensile stress is 199 MPa and it is located near the center of weld FZ.

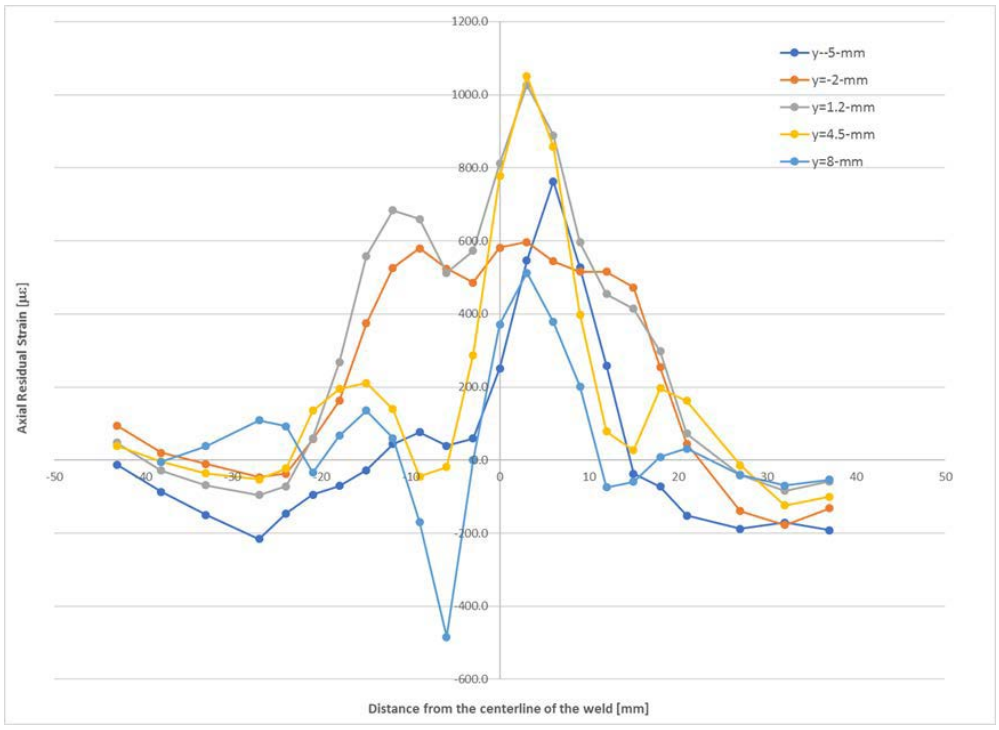

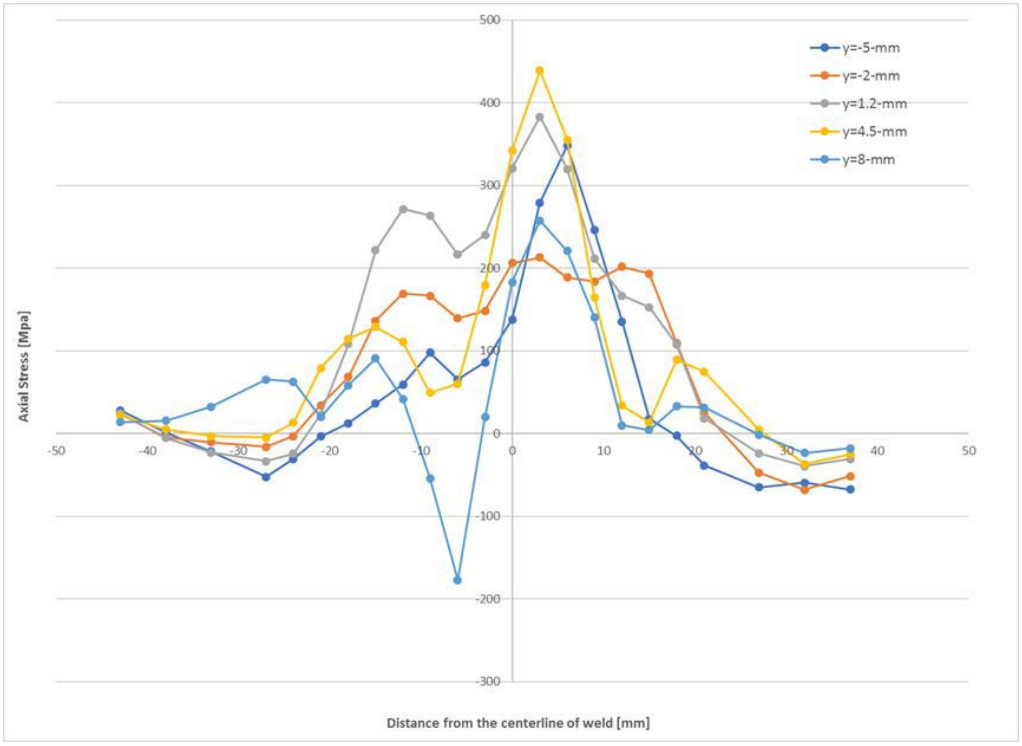

Figure 17 Measured residual strain plot and the estimate residual stress plot, along the five scanned contours in the axial direction. The maximum value of the residual tensile stress is 439 MPa, and it is located near the center of weld FZ.

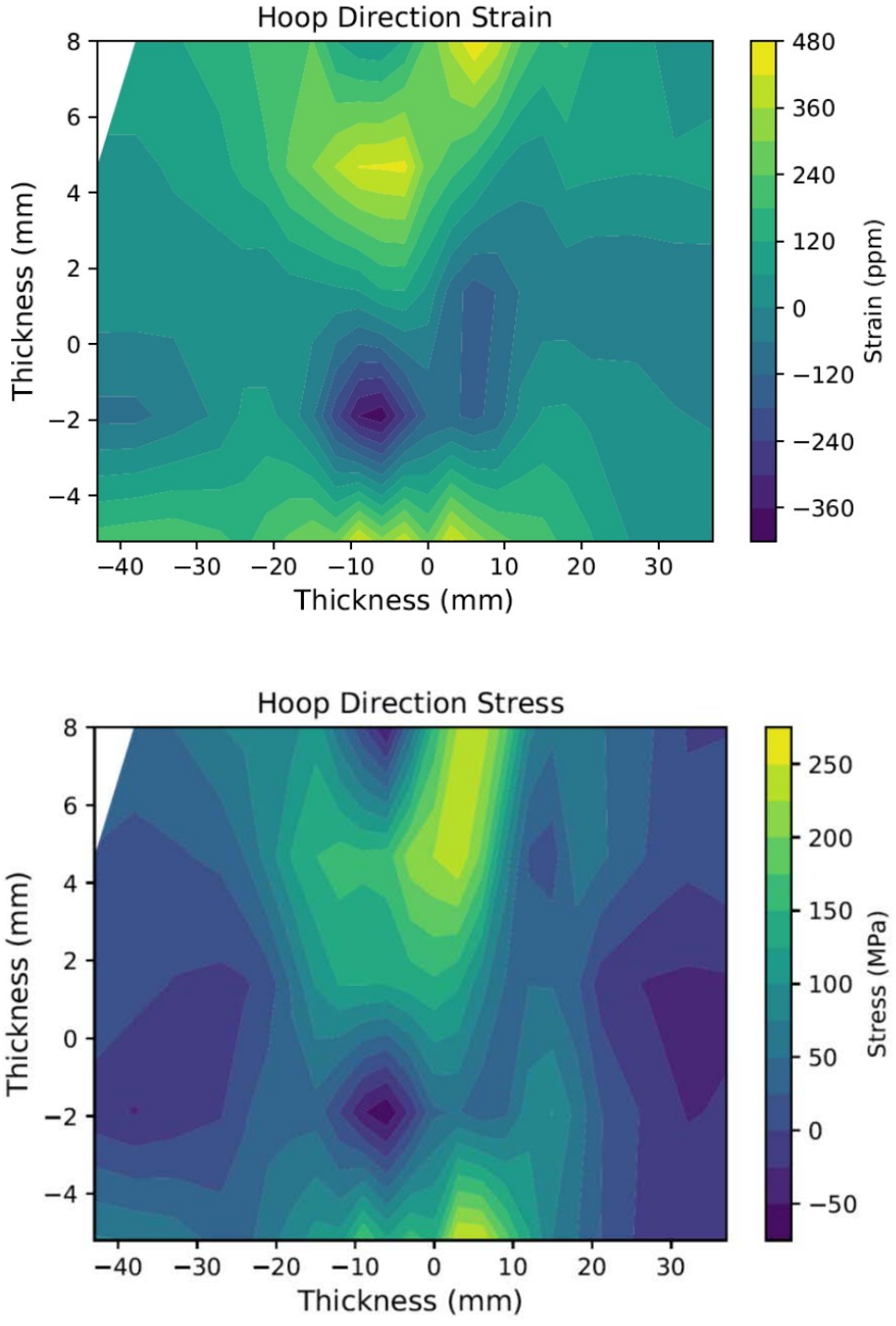

Figure 18 2-D strain and stress contour plots in Hoop direction.

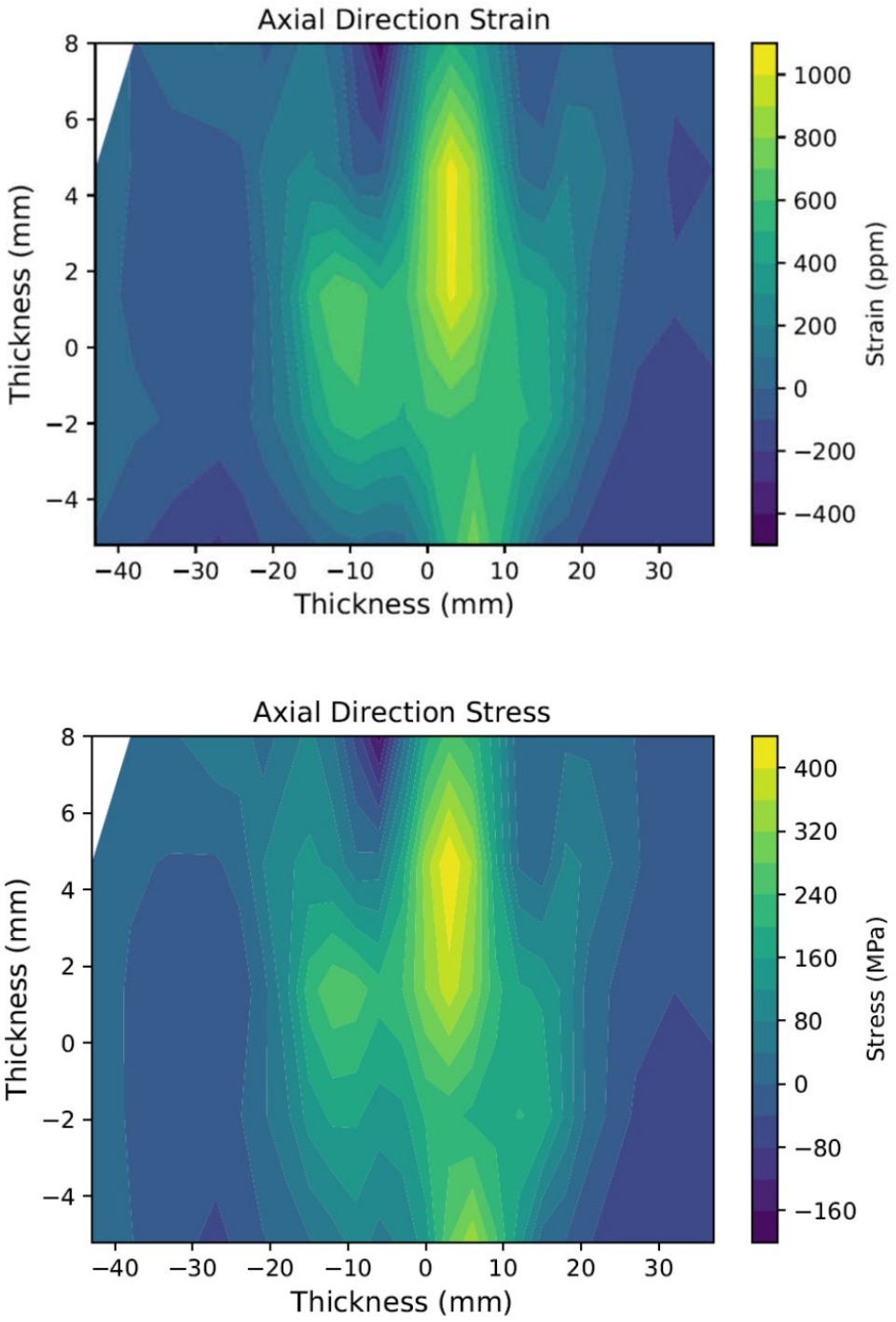

Figure 19 2-D strain and stress contour plots in Axial direction.

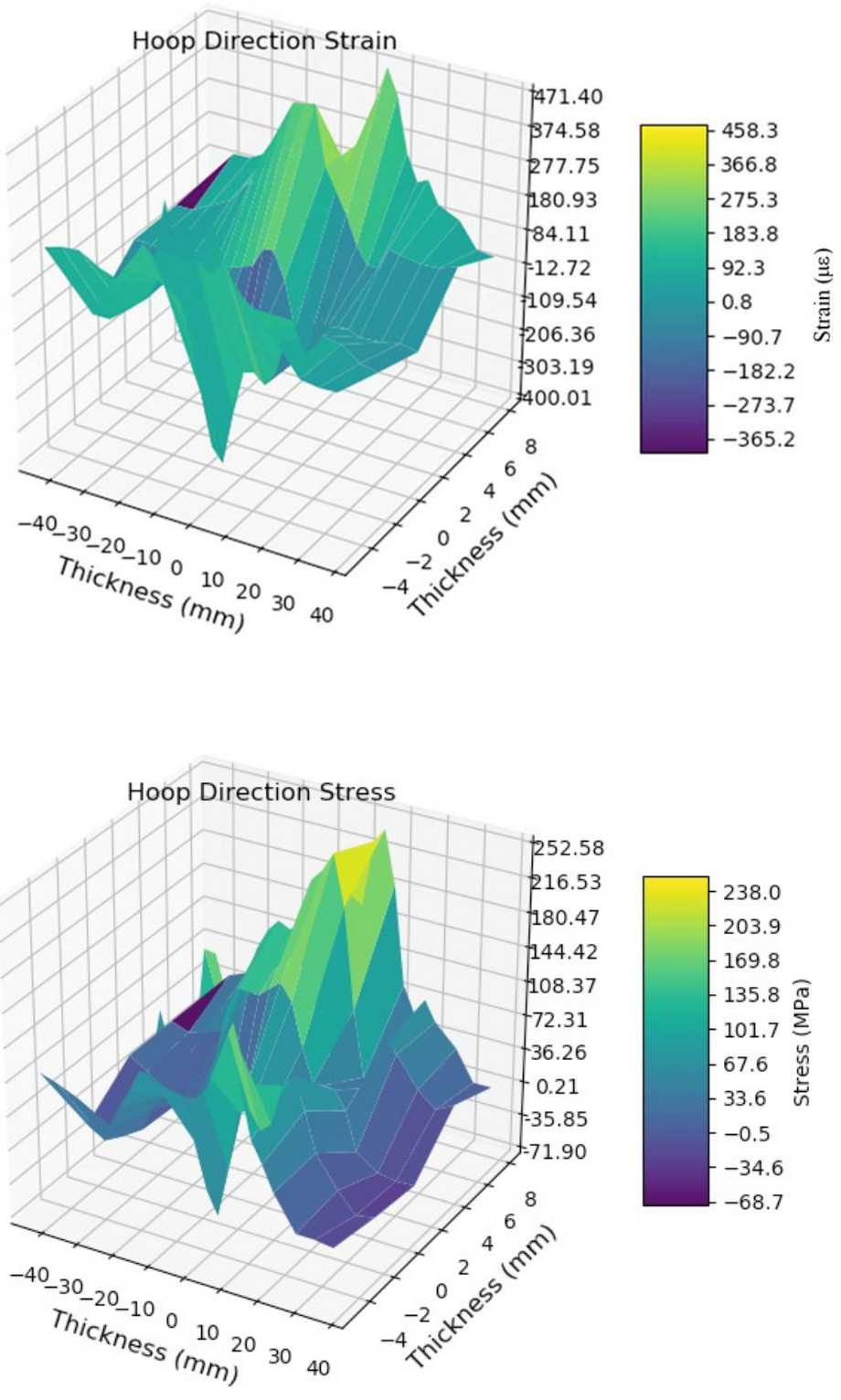

Figure 20 3-D strain and stress contour plots in Hoop direction.

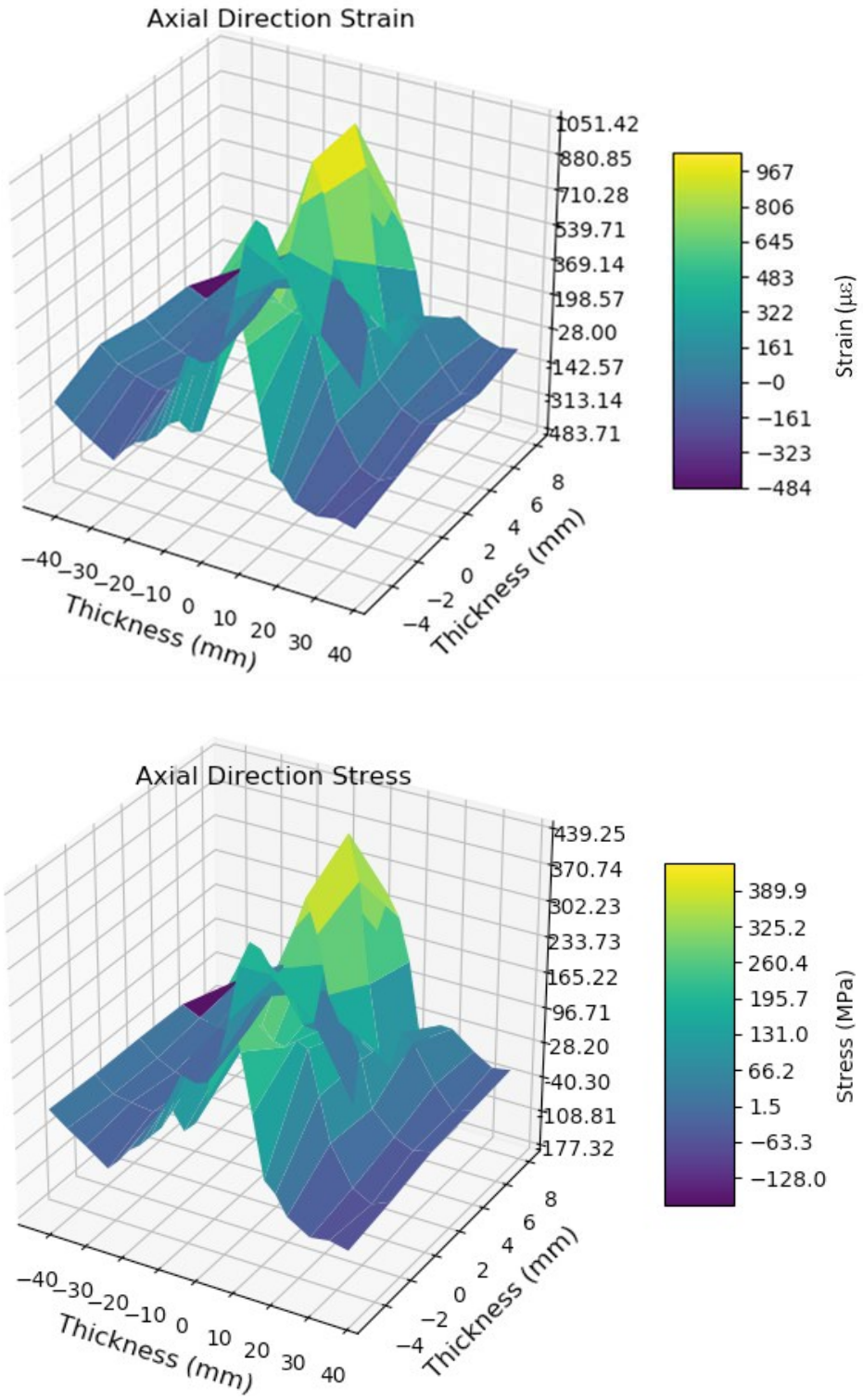

Figure 21 3-D strain and stress contour plots in Axial direction.

Also note that the final weld passes were sometimes offset from the centerline of the weldment, yielding an asymmetric appearance.[1] This phenomenon was also observed from the shift of the maximum stress profile to the right of the centerline of the weld, from the residual stress plots. Furthermore, Figures 15-17, it also show the relative shift of the stress or strain profiles in the fusion zone along the different scanned contours. This observation is also consistent with the misalignment of the fusion zones at outer diameter and the inner diameter of the weld FZ, as shown in Figure 22. Moreover, there is a potential outlier with high compressive stress of 177 MPa located at FZ, as shown in Figure 17, of the axial residual stress profile along the scanned contour near the OD surface, i.e., at the contour of y = 8-mm. This phenomenon could be the result of impurity, or manufacturing processing observed from grinding and machining marks associated with the longitudinal weld at FZ. This mechanical treatment can significantly impact the near surface stresses associated with the processed regions.

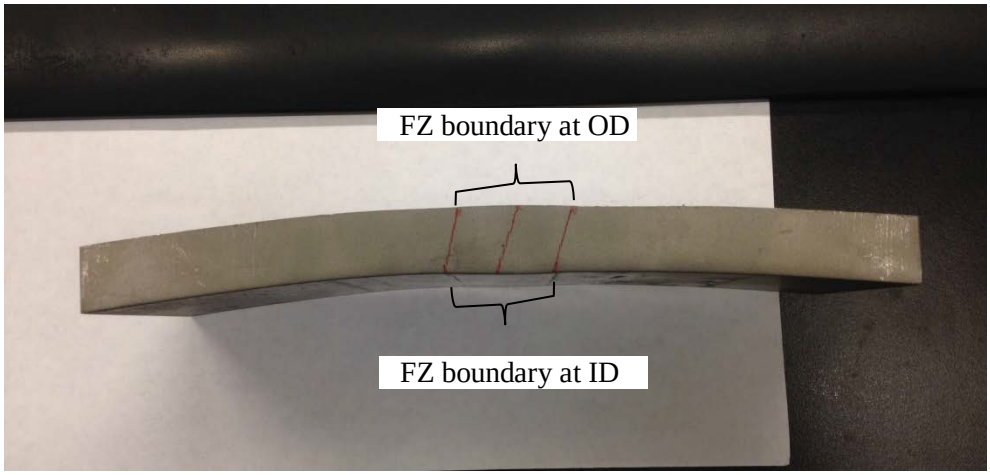

(a)

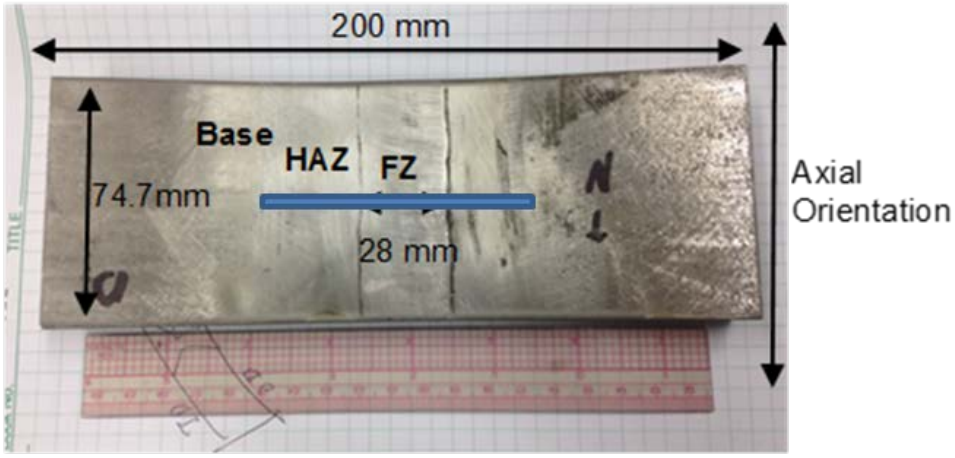

(b)

Figure 22 (a) Misalignment of the fusion zone centerline and boundary along the OD and ID of the weldment, (b) Neutron scanned zone was marked with blue strip.

5. CONCLUSION

Residual strains have been measured by neutron diffraction and interpreted in terms of residual stresses in a stainless steel longitudinal welded plate removed from a Sandia mockup canister. The general observations from the neutron residual stress mapping study on the received Sandia mockup weld plates are as follows.

1. The maximum tensile residual stress of 439 MPa, located in FZ orientated in the axial direction, is much higher than the yield stress of 200 MPa for the 304L and 308L SS metals; and it is expected to above the yield stress of the weld.[10, 11] Furthermore, based on Lincoln SAW 308/308L weld,[12] the yield stress and UTS for 308/308L weld are 380 MPa and 565 MPa, respectively. The residual axial tensile stress, which is shown in Figure 16, also indicates that tensile stresses exist throughout the thickness of the weldment in the FZ, including HAZ region up to 10-mm away from the weld toe (i.e., the edge of FZ), and the associated maximum axial tensile residual stress is at 272 MPa.
2. The maximum hoop tensile residual stress has a value of 253 MPa and it is located in FZ near OD surface and near ID interior of y=-5-mm contour. The residual hoop tensile stress is shown in Figure 14 and it also indicates that tensile stresses exist throughout the thickness of the weldment in FZ, including HAZ region. Moreover, the maximum hoop tensile stress at HAZ region is at 162 MPa.
3. The maximum radial tensile stress is at 200 MPa in FZ and the tensile stress field is also throughout the thickness of the FZ and HAZ regions. The maximum tensile stress at HAZ region is at 115 MPa.
4. From the above observations, the residual stress profiles estimated from ORNL neutron diffraction technique and Sandia deep hole drilling approach are in good agreement.
5. The received weldment sample was cut out from the parent mockup canister wall of Section B; but it is believed that a significant redistribution and relaxation of residual stress occurs during the cutting process. For instance, the received sample lost some of its curvatures, and the consequence is the reduced strain level. Such as that we observed from the radial strain measurement of near zero value, which indicates that the radial stresses had been redistributed. In the same token, when the canister cylinder wall was cut, the hoop stresses were also relaxed as well as that of the axial stresses. Nevertheless, a significant amount of residual stresses remained in the weldment.

References

[1] D.G. Enos and C.R. Bryan, Final Report: Characterization of Canister Mockup Weld Residual Stress. Sandia National Laboratory, November 22, 2016. FCRD-UFD-2016-000064.

[2] Nuclear Waste Technical Review Board (NWTRB). (2010). Evaluation of the technical basis for extended dry storage and transportation of used nuclear fuel. Arlington, VA. Nuclear Waste Technical Review Board.

[3] Hanson, B., Alsaed, H., Stockman, C., Enos, D., Meyer, R. and Sorenson, K. (2012). Gap analysis to support extended storage of used nuclear fuel, FCRD-USED-2011-000136. U.S. Department of Energy.

[4] NRC. (2012a). Identification and Prioritization of the Technical Information Needs Affecting Potential Regulation of Extended Storage and Transportation of Spent Nuclear Fuel. Draft for comment. U.S. NRC.

[5] Potential Chloride Induced Stress Corrosion Cracking of Austenitic Stainless Steel and Maintenance of Dry Cask Storage System Canisters. Washington, D.C.: U.S. NRC.

[6] Extended Storage Collaboration Program (ESCP) Progress Report and Review of Gap Analyses. Palo Alto, CA.

[7] Enos, D. G., Bryan, C. R. and Norman, K. M. (2013). Data Report on Corrosion Testing of Stainless Steel SNF

Storage Canisters, FCRD-UFD-2013-000324. U.S. DOE, Office of Used Nuclear Fuel Disposition.

[8] Bryan, C. R. and Enos, D. G. (2015). Analysis of Dust Samples Collected from an Unused Spent Nuclear Fuel Interim Storage Container at Hope Creek, Delaware, SAND2015-1746. Albuquerque, NM. Sandia National Laboratories.

[9] Stainless Steels Properties – How to Weld Them and Where to use Them. The Lincoln Electric Company. http://www.lincolnelectric.com/assets/global/Products/Consumable_StainlessNickelandHighAlloy-Excalibur-Excalibur316316L-17/c64000.pdf

[10] D. Dean, and M. Hidekazu, "Numerical simulation of temperature field and residual stress in multi-pass welds in stainless steel pipe and comparison with experimental measurements", Computational Materials Science, 37, 269-277 (2006).

[11] Joshua Kusnick, Michael Benson, and Sara Lyons, Finite Element Analysis of Weld Residual Stresses in Austenitic Stainless Steel Dry Cask Storage System Canisters Technical Letter Report. December 2013. NRC report, ADAMS ML13330A512.pdf.

[12] http://www.lincolnelectric.com/assets/global/Products/Consumable_StainlessNickelandHighAlloy-Lincolnweld-Lincolnweld308308L/c61024.pdf.